Monte Carlo simulation for seismic analysis of a long span suspension bridge

L. Sgambi [a,*], E. Garavaglia [a], N. Basso [b], F. Bontempi [c]

[a] Department of Civil and Environmental Engineering, Politecnico di Milano, Milan, Italy
[b] Department of Architecture, Tokyo Denki University, Tokyo, Japan
[c] Department of Structural and Geotechnical Engineering, University of Rome La Sapienza, Rome, Italy

1. Introduction

The seismic analysis of complex structures is generally a problem affected by uncertainty. Some of the most important uncertain parameters are: the location of the epicenter, the seismic intensity and the attenuation law, the velocity of seismic waves through the soil, the frequency content of the seismic waves, the local effects of the site, etc. Aside from these uncertainties, typical of the seismic analysis of any structure, there are also the uncertainties and non-linearities of behaviour typical of the complex structures such as long-span suspension bridges [1,2]. Many uncertainties are related to the composition of the soil, some are related to the structural behaviour, i.e. the real distribution of masses and rigidity, and others to the numerical models used to describe it.

For a so an extensive structure such as a long-span suspension bridge, complete knowledge of the soil besides being extremely expensive for such an extensive structure, does not introduce the seismic analysis into the well-structured problems defined by Simon [3] since a certain amount of uncertainty would remain within the problem. Remaining with seismic matters, it seems in fact impossible to predict with precision the real location of the epicentre or the prevailing direction of seismic waves.

From a general point of view, the uncertainties can be divided into three fundamental types: *aleatory uncertainties* (arising from the unpredictable nature of the size, the direction or the variability of environmental action, the parameters estimation), *epistemic uncertainties* (deriving from insufficient information as well as from measurement errors or inadequate modelling) and *model uncertainties* (deriving from the approximations present in numerical models). The characterization of uncertainties in engineering and their treatment within structural problems is an extremely wide theme; Der Kiureghian and Ditlevsen [4] provide an interesting overview of this topic. In general, random or aleatory uncertainties can be addressed using a reliable procedure to estimate the parameters involved in the problem [5–8]. Epistemic uncertainty can be reduced by improving the surveys aimed at characterization of the phenomena studied and using fuzzy approaches [9–11]. Finally, one possible way to reduce model uncertainties is the use of several FEM models with different levels of detail and the proper planning of numerical simulations [12,13].

In this context, it is evident that a classic deterministic approach is inadequate for an appropriate assessment of the behaviour of a long-span suspension bridge under seismic action. More reliable approaches can be found in methods to handle uncertainties in structural problems, such as using probabilistic formulations or fuzzy theories.

* Corresponding author. Address: Department of Civil and Environmental Engineering, Politecnico di Milano, Piazza Leonardo da Vinci 32, 20133 Milan, Italy. Tel.: +39 02 2399 4212; fax: +39 02 2399 4312.

E-mail address: luca.sgambi@polimi.it (L. Sgambi).

2. Structure description

The structure analysed in this article shows geometric and mechanical characteristics based on the design of the bridge over the Strait of Messina Bridge in 1992 [14]. Although the structure was not built, the project and the analyses are of great interest due to the importance of the construction and the problems involved in the definition of structural behaviour. The project of 1992 provides that the Strait is crossed with a suspended bridge with a main span of 3300 m in length (Fig. 1). The total length of the bridge deck, including the side spans, is 3666 m, with a width of 52 m. The bridge deck is constituted by three box sections (Fig. 2), the external ones with the task of carrying roadways and the central one the railway system. Every 30 m the three box sections are joined by a transverse beam. The shape of the box sections and the distance that separates them were designed to reduce the effect of wind on the structure. The longitudinal profile of the bridge deck is slightly arched, starting from an altitude of 52 m on the side of Sicily, rising to 77 m in the middle of the bridge and then dropping to 62 m on the side of Calabria. This trend is to ensure a minimum clearance of 60 m with a width of 600 m, which is necessary for navigation.

The two towers (Fig. 3) of the suspension bridge (made entirely of steel) are two multilevel portal frames and reach an altitude of 381 m. The legs are not perfectly vertical but have a transversal inclination of approximately 2° so that the distance between the axes of the legs change from approximately 78 m at the base to 52 m at the top. The leg sections are octagonal and can be fitted within a rectangle of 16×12 m. The two legs are connected by 4 transverse beams that mount the structure, approximately 17 m high and 4 m wide. The structure has four main cables, arranged in pairs on the vertical side of the ends of the transverse beams of the bridge deck, and thus at a distance of 52 m. The axle spacing between the cables of each pair is 1.75 m and each cable has a diameter of approximately 1.24 m. The effective development of

the cables is approximately 5240 m and includes 3370 m of cable length in the central span and 1020 m and 850 m on the two side spans. The two cables of each pair are connected to each other every 30 m by steel rings from which hangers extend to connect and support the bridge deck to the main cables.

The main cables supporting the floor transmit their axial action in part along the vertical parts of the towers, and in part directly to the ground, anchored in two large structures (on the side of Sicily and Calabria), in massive reinforced concrete. The anchor blocks are different, since the nature of the deposit on which they rest is diverse. In Sicily, the land is made up of slightly cemented gravels while in Calabria there is a more consistent rock. For this reason the anchoring in Sicily is composed of a block of approximately 328,000 m^3 while that in Calabria is approximately 237,000 m^3. Table 1 shows the main mechanical characteristics of the structure.

The main structure of the bridge (except for the anchoring blocks) is designed in steel. The characteristics of strength and deformability are shown in Table 2.

3. Definition of seismic input

3.1. Signal generation

For the analysis of structures resistant to seismic action, a dynamic analysis of response (using a response spectrum or a time history) is often required by the technical rules. This analysis is required for all structures that have high non-linearities of behaviour, when structures to be analysed have irregularities in plan or in elevation, or when certain temporal information in the response of the structure itself must be known [15]. In some cases the most appropriate dynamic analysis is the step-by-step integration of the equations of motion characterizing the seismic event. However, the use of dynamic analysis is linked to the need to have an accelerogram representative of the seismicity of the area, data that is not always present. Besides, a non-deterministic approach would
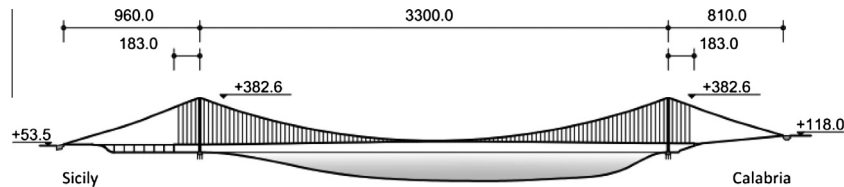

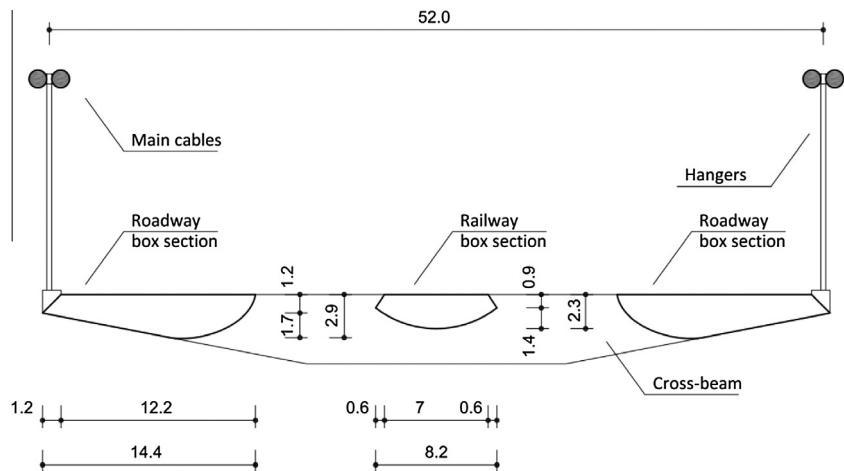**Fig. 1.** Geometrical dimensions of the Messina Strait Bridge (m).

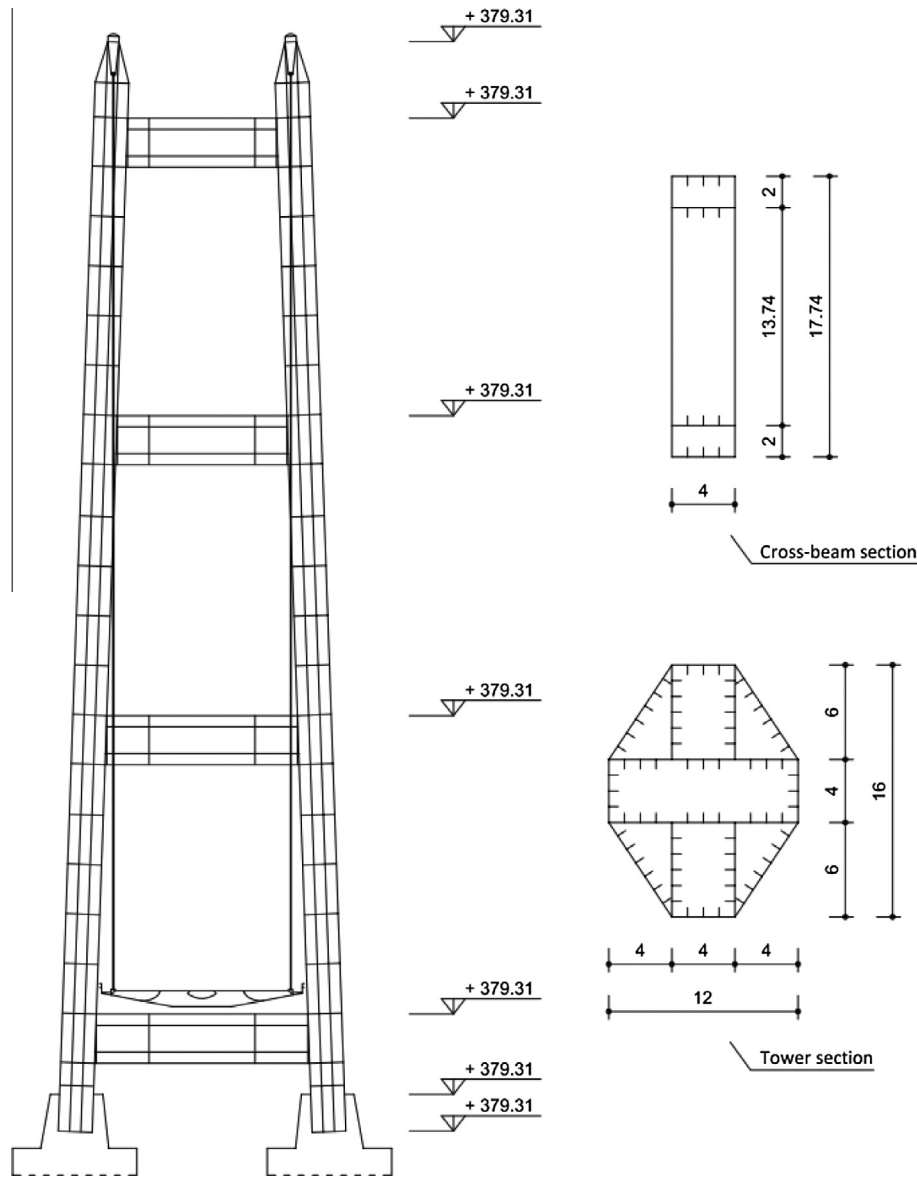**Fig. 2.** Geometrical dimensions of the bridge-deck section (m).

Fig. 3. Geometrical dimensions of the towers (m).

Table 1
Main physical property of the elements constituting the structure of the bridge.

Element	Area (m^2)	I_{tors} (m^4)	$I_{bend,1}$ (m^4)	$I_{bend,2}$ (m^4)
Main cable	2.02	0.6494	0.3247	0.3247
Hangers close to the tower	0.0327	1.700E−04	8.510E−05	8.510E−05
Hangers close to the quarter of the bridge	0.0117	2.180E−05	1.090E−05	1.090E−05
Hangers close to the centre of the bridge	0.0137	2.987E−05	1.493E−05	1.493E−05
Tower legs	8.4252	52.941	222.3904	131.5288
Transverse beams	1.9792	13.9804	67.2698	6.1036
Roadway box section	0.45	1.1642	0.3589	8.0787
Railway box section	0.2996	0.6877	0.2245	2.4394
Transverse beams	0.3233	1.1344	0.6336	0.7629

provide for the use of a large number of numerical simulations, requiring a number of events of certain importance undoubtedly superior to the number of events recorded to date in the proximity of the construction site.

There is a clear need to be able to build artificially the temporal histories representative of the seismicity in a given area. In this case it is important that the artificial temporal history is consistent with the seismicity of the region and representative of the earthquake expected or defined by technical regulations. It is well known, in fact, that the physical conditions of the site taken into consideration affect the characteristics of the seismic event [16,17]. The duration of the event, the frequency content of the signal and the intensity of the earthquake are strongly affected by several geological parameters such as the mechanical

Table 2
Mechanical properties of the steel.

Element	Young's modulus (MPa)	Yielding strength (MPa)	Ultimate strength (MPa)
Cable	190,000	1400	1800
Towers and bridge deck	210,000	355	510

characteristics of the soil, the geometric shape of the surface, the distance of the source, and the fault mechanism.

The artificial seismogram can be obtained in different ways [18]:

1. by selecting and properly modifying real accelerograms;
2. by generating artificial accelerograms based on a model of the seismic source;
3. by generating artificial accelerograms compatible with a response spectrum of the project.

However, none of the above is exempt from errors or approximations with respect to a natural seismic event.

With regard to the first method, Duglas [19] shows how many of the real accelerograms are affected by recording errors: insufficient digitizer resolution, S-wave trigger and insufficient sampling rate are the most common causes of non-standard errors in the recording of seismic motion. Boore and Bommer [20] also highlight how experimental measurements from which artificial accelerograms are often obtained could be affected by distortions and shift of the baseline of reference, from which non-realistic diagrams of velocity and displacement are derived. Therefore, Boore and Bommer propose using a baseline correction method to resolve this type of error (for more details [20]).

Different major models of the seismic event source are discussed in Liu and Liu [21] that could be widely used for seismology studies and earthquakes prediction. However, such models are usually based on assumptions that simplify the seismic problem. For example, in many models that are valid from an engineering perspective, the source is considered localized in a single point. It appears evident that such models will be all the more approximate the more the actual source assumes the character of a line or a surface with respect to the observation point.

In this work the third approach is used, artificially generating accelerograms compatible with a design spectrum. Such approach has been studied by many researchers and there are several methods in the literature used to obtain the spectrum-compatible accelerograms [22–27]. Such methods are essentially numerical and will produce accelerograms with spectra that approximate the design spectrum according to a certain user-defined tolerance.

From the analysis performed, the authors propose the application of the methodology referred in the previous point 3 that is the generation of artificial accelerograms compatible with a design response spectrum, as explained in Section 4.2.

3.2. Spatial variability

A long-span suspension bridge is a very extensive structure. This implies that the geological conditions can vary considerably from one support to another one. The effect of the geologic variability and uncertainty involved in the seismic problem usually leads to a loss of coherence of the seismic signal [28–33]. Wang et al. [34] studied the effect of the loss of coherence of the signal and the time of propagation of the seismic wave in the ground on the Jiangyin Yangtse River Bridge, a long-span suspension bridge of 1385 m by means of random vibration analysis. The authors conclude that the dynamic response of the towers is

dominated by the seismic excitation at the base of the same and that the error committed by a modelling that does not consider the coherence of the signal between the two sides of the bridge is less than 15%, acceptable for an engineering application. Similar results were also obtained by Soyluk and Dumanoglu [35] who compared the dynamic response of a cable-stayed bridge equal to 344 m using an asynchronous dynamic analysis which took into account the delay due to the seismic excitation resulting from wave propagation in the ground and a stochastic approach that is able to consider the coherence of the signal but not the delay of the wave. The same authors show how the shear forces in the deck and towers are higher for the analyses carried out using the asynchronous approach. They attributed such differences to the modelling of the delay of the seismic excitation due to finite velocity of the wave propagation in the ground. In fact, by increasing the velocity of the seismic wave the authors show how the differences between the two models produce increasingly similar results.

Continuing with the topic of spatial variability of the signal and loss of coherence of the same, it is worth mentioning the study carried out by Boissières and Vanmarcke [36] who studied the spatial correlation with regard to 12 seismic events using a non-parametric method called multidimensional correlation mapping. The seismic events analysed originated from SMART1 accelerogram array able to record the seismic event on a square area of 4000×4000 m. Their analyses show that the correlation of seismic movements along the territory varies considerably according to the event being studied. In general, the correlation appears to be more significant on the displacements relative to accelerations, moreover for many events the correlation seems to be strongest along the epicentral direction rather than along the transverse direction. From the maps of correlation reported in their article it can be noted how the correlation factor (set equal to 1.0 in the centre of the array) decreases to average values of 0.25 on the boundary of the squared area being examined (2000 m from the centre of the array) with a number of peaks of 0.7 and many areas of the surrounding area with correlation values below 0.1.

On the basis of these considerations and taking into account the large size of the structure, the seismic analysis is carried out considering an asynchronous seismic input. Different displacement time histories are applied at the connection points between the structure and the ground.

4. Seismic analysis of a long span bridge

4.1. Definition of the numerical model

With regard to the analysis of the seismic behaviour of the bridge, a numerical model was developed that considers the three-dimensionality of the structure in order to be able to also consider transverse or torsional movements. For structural analysis, the ADINA [37] software code was used coupled with a code written in FORTRAN able to conduct probabilistic seismic analyses and to interpret the results obtained automatically [1,38–40].

The numerical model consists of 1593 finite elements of the Hermite's two node beam type with six degrees of freedom per node. The total number of degrees of freedom used by the model is 6678. Analyses are developed in the field of large displacements and of small strains. Fig. 4 reports the image of the model and the measurement points of the bridge deck displacement.

4.2. Definition of seismic input

The need to carry out a high number of analyses requires a large number of seismic scenarios. As such, a database of artificial accelerograms was created through the well-known SIMQKE code
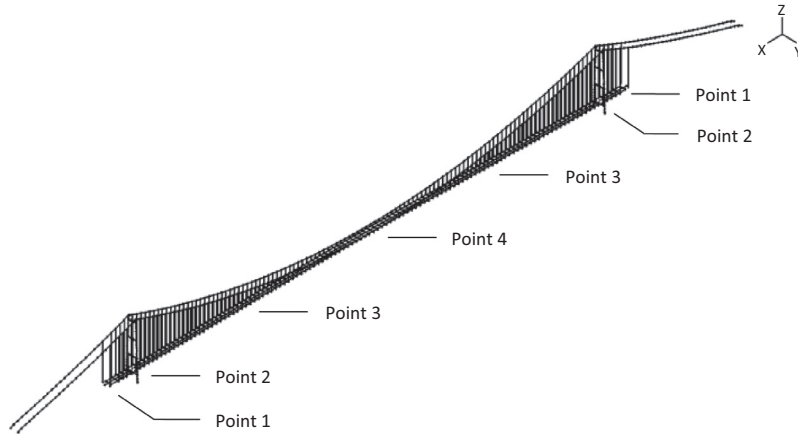
Fig. 4. Numerical model of the bridge and measurement points for the displacement of the bridge deck.

developed by Gasparini and Vanmarke [41] that allows the artificial creation of a preset number of statistically independent accelerograms referring to a specified response spectrum. In short, the artificial accelerogram is generated as a summation of sine wave functions:

$$Z(t) = I(t) \cdot \sum_n A_n \cdot \sin(\omega_n \cdot t + \Phi_n) \qquad (1)$$

where A_n represents the width of frequency oscillation ω_n. The values of A_n are optimized during the process of seismic generation in order to obtain an accelerogram with response spectrum that is close to that defined by the user. The angles Φ_n represent the phase angles and are chosen at random, while with $I(t)$ an envelope law is indicated, necessary to model the increasing, steady and decreasing phases of the seism.

Using this procedure it is possible to obtain a suitable number of accelerograms defined as spectrum-compatible to simulate the seismic event. These accelerograms were subsequently integrated to obtain temporal histories of displacement. In general, the direct integration of the accelerograms leads to non-realistic displacement time histories with the phenomena of "shift" on final velocity and final movements, an error similar to the one highlighted by Boore and Bommer [20] concerning artificial events obtained with real seismic events. This phenomenon, although not realistic, does not affect the results of seismic analyses with synchronous scenarios [42]. Displacement time histories, or accelerograms, are in fact applied to the structure with the aim of giving to the mass an inertial load. Even though the points of application undergo a final unrealistic shift, this cannot affect the relative displacements and internal actions involved. However, in the event of seismic analysis with asynchronous scenarios, a shift on displacements in different parts of the structure can lead to structural behaviours that are drastically incorrect [43]. For this reason, in this paper, the seismic events generated artificially through the SIMQKE code have been corrected by the baseline method. It is important to point out that the SIMQKE code used to artificially generate accelerograms has an internal method of baseline correction in order to generate accelerograms that, once integrated, provide a final zero velocity. However, it was found that numerical errors due to the process of numerical integration lead to shifts both in terms of ultimate velocities and in terms of ultimate displacements.

It was found that the magnitude of the shift to be made in the correction decreases by increasing the precision with which the numerical integration is carried out (trapezoidal method, the method of Cavalieri–Simpson, Weddle's method). However, a significant shift is still present. Therefore, a further correction was carried out on the artificial accelerograms in order to physically

obtain a correct recording of the displacements of the ground during seismic events. With this procedure a database of 400 time histories of spectrum-compatible displacement was then created.

4.3. Preliminary modal analysis

The Figs. 5–7 show the results of a modal analysis that is preliminary to seismic analysis. The modal participation factors are marked as points along a surface having the period of vibration along the axis of the x-axes. The elastic response spectrum of the area where the presence of the bridge is foreseen is overlapped at the set of points representing the modal participation factors. In this way it is possible to visually note the influence of vibration modes of structure with regards to seismic action. Figures show that almost all modes of vibration that involve great quantities of mass are external to the part of elastic response spectra with higher values of acceleration. The only mode of vibration that involves a certain quantity of mass and that is located in the central part of the spectrum of response spectrum can be seen in Fig. 7 and is a longitudinal vibration. The fundamental period of vibration is 32 s and can be seen in Fig. 6.

4.4. Probabilistic seismic analysis

Considering the remarkable distances between the points of support (960 m – 3300 m – 810 m) and the lack of information about the characteristics of the soil along the area of development of the structure, the seismic action was considered asynchronous
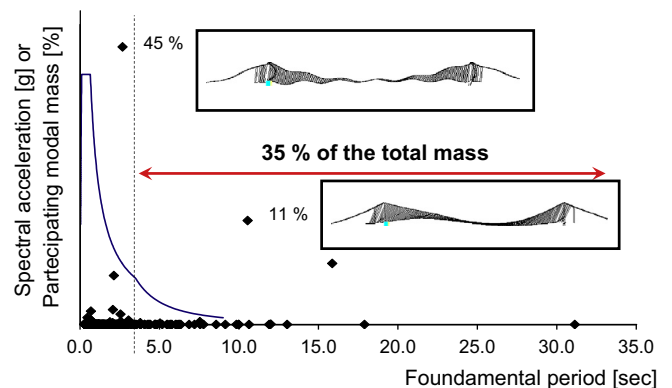

Fig. 5. Representative points of the modal participation factors and principal deformation modes for the vertical direction.
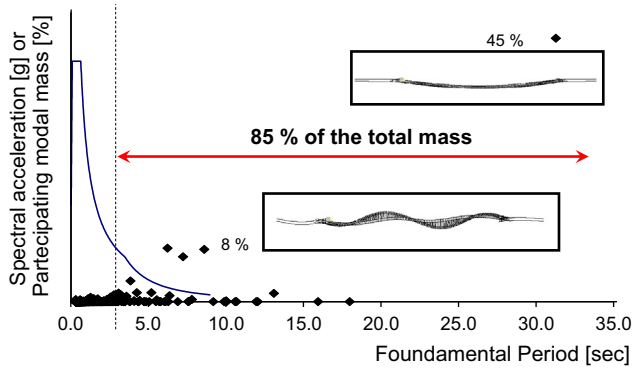
Fig. 6. Representative points of the modal participation factors and principal deformation modes for the transversal direction.
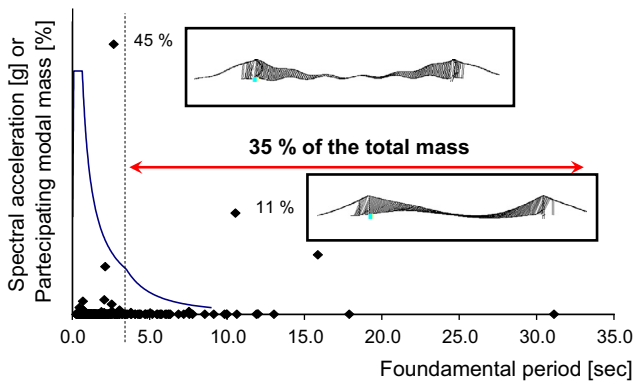

Fig. 7. Representative points of the modal participation factors and principal deformation modes for the longitudinal direction.

and was simulated using a series of displacement shifts defined as in the previous paragraphs, applied to the six areas in which the bridge comes into contact with the ground (anchor blocks, tower supports and terminal segment of the bridge deck) as can be seen in Fig. 1. Considering the significant uncertainties present, the seismic analysis was carried out through a Monte Carlo simulation, performing 50 seismic analyses and obtaining, in his way, a number of statistical indices such as the average, the fractile at 95% and the variance of results. The histories of displacement were applied to the various areas with a random time delay varying in a range between 0 and 4 s between the points of contact with the ground. Distributions of uniform probabilities were attributed to the database containing the time histories of displacement as well as to the temporal variable indicating the delay of the seismic action.

The structure was subject to three Monte Carlo simulations with seismic scenarios having different values of the peak ground acceleration (PGA). 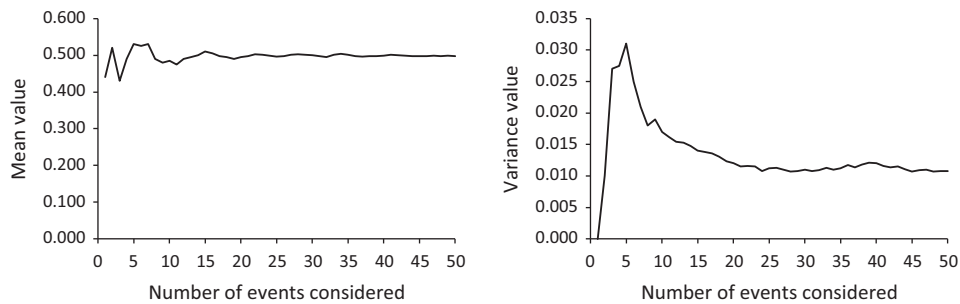Considering a conventional service life of the bridge of 200 years, three different scenarios can be considered: a first scenario with PGA = 1.80 m/s^2 (earthquake with a return period of 50 years), a second scenario with PGA = 2.60 m/s^2 (earthquake with a return period of 400 years) and a third scenario with PGA = 5.70 m/s^2 (earthquake with a return period of 2000 years). For the first scenario ("normal" scenario) the conditions for the normal functioning of the work must be guaranteed and the structural checks must remain within the elastic range. For the second scenario ("exceptional" scenario) interruptions due to temporary repairs can be accepted, the major parts of the bridge must be verified in the elastic range. For the third scenario ("extreme" scenario) an interruption of service for a lengthy period due to major repairs is permitted but the main parts of the bridge should not suffer a collapse.

The results reported in this work refer to a number of specific measurement points that are:

- Longitudinal displacement of the bridge deck at the expansion joint (point 1 in Fig. 4).
- Transverse displacement of the bridge deck near the tower legs (point 2 in Fig. 4).
- Vertical and transverse displacement of the bridge deck at a quarter of the bridge (point 3 in Fig. 4).
- Vertical and transverse displacement of the bridge deck at the centre of the bridge (point 4 in Fig. 4).

From Figs. 9–13 the results in terms of displacement of the analyses performed for the selected measurement points are shown. These values are reported in tabular form for the three seismic intensities previously defined. The two right-hand columns of the figures in question also indicate the relationships between the various parameters relating to different seismic intensity in order to verify the increase of displacement on the magnitude depending on the seismic intensity. To point out how uncertainties affect the parameters of displacement analysed, the results will be reproduced also in terms on distribution of probability, using normal distributions.

In addition to these kinematic quantities, Figs. 14 and 15 report the levels of the stress present in the towers and cables.

Assuming the seismic event with PGA of 1.80 m/s^2 as reference earthquake, it is possible to note that the earthquake with PGA of 2.6 m/s^2 has a seismic action 1.44 times higher, while the earthquake with PGA of 5.70 m/s^2 is equal to an earthquake that is 3.17 times stronger. These values will be useful to perform certain observations on the impact of uncertainties examined, during the seismic motion.

4.5. Discussion of results

It can be inferred from the analysis how the variable representing the average displacement has a very good convergence, by which 20 sets of analyses are sufficient to describe its values in a
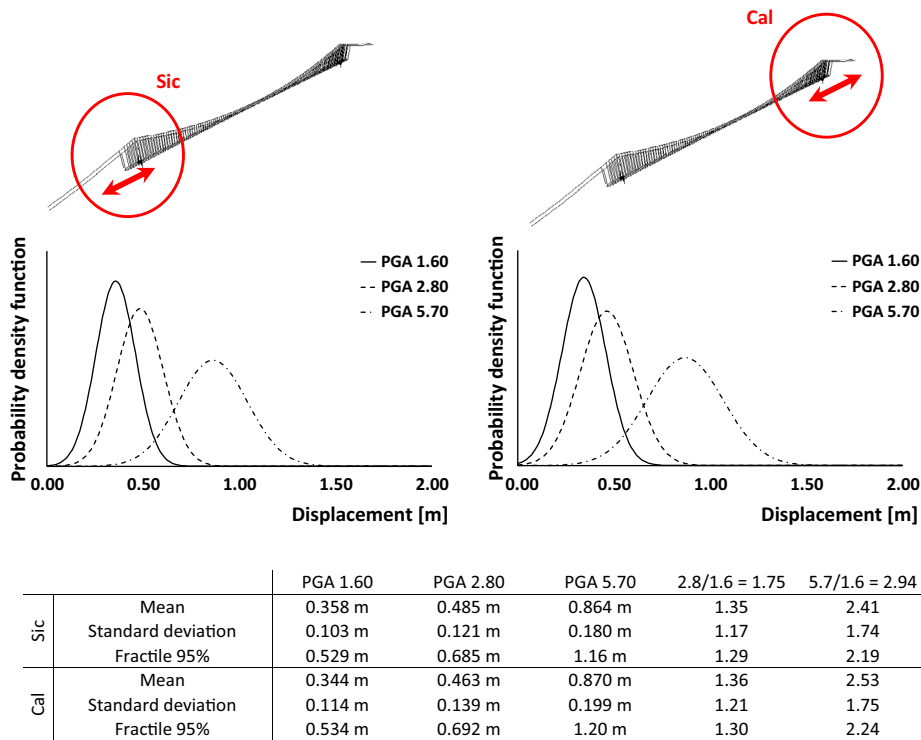

Fig. 8. Trend of the mean and variance of the transversal displacement at quarter of the bridge, Calabria's side.

		PGA 1.60	PGA 2.80	PGA 5.70	2.8/1.6 = 1.75	5.7/1.6 = 2.94
Sic	Mean	0.358 m	0.485 m	0.864 m	1.35	2.41
	Standard deviation	0.103 m	0.121 m	0.180 m	1.17	1.74
	Fractile 95%	0.529 m	0.685 m	1.16 m	1.29	2.19
Cal	Mean	0.344 m	0.463 m	0.870 m	1.36	2.53
	Standard deviation	0.114 m	0.139 m	0.199 m	1.21	1.75
	Fractile 95%	0.534 m	0.692 m	1.20 m	1.30	2.24

Fig. 9. Longitudinal displacement of the bridge deck at the expansion joints.

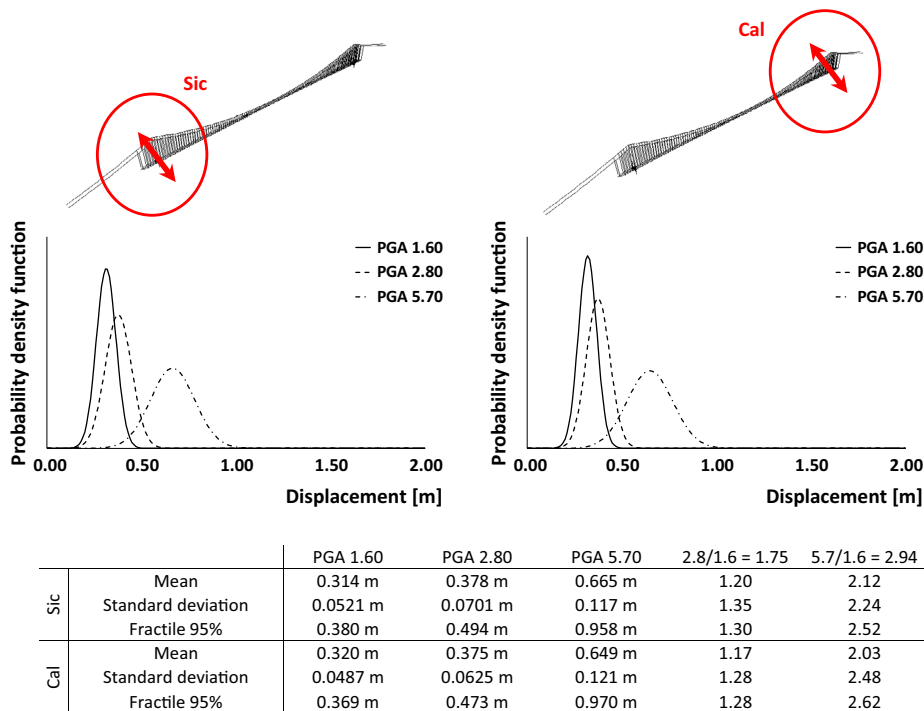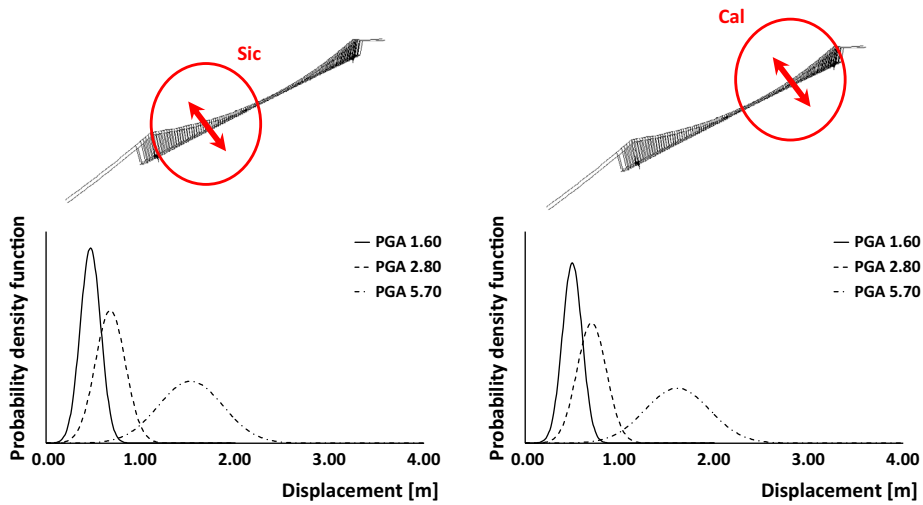|		PGA 1.60	PGA 2.80	PGA 5.70	2.8/1.6 = 1.75	5.7/1.6 = 2.94
Sic	Mean	0.314 m	0.378 m	0.665 m	1.20	2.12
	Standard deviation	0.0521 m	0.0701 m	0.117 m	1.35	2.24
	Fractile 95%	0.380 m	0.494 m	0.958 m	1.30	2.52
Cal	Mean	0.320 m	0.375 m	0.649 m	1.17	2.03
	Standard deviation	0.0487 m	0.0625 m	0.121 m	1.28	2.48
	Fractile 95%	0.369 m	0.473 m	0.970 m	1.28	2.62

Fig. 10. Transverse displacement of the bridge deck near the tower legs.

correct manner. The variable that represents the variance of distribution instead has a slower and more irregular convergence by which also 50 analyses can, in some cases, be insufficient to reproduce its value correctly (Fig. 8). The results, in terms of variance, reported in the following diagrams are therefore less accurate than the results presented in terms of average value.

Figs. 9–13 report the results in terms of displacement ("Sic" stands for "Sicily side" and "Cal" stands for "Calabria side"). While for seismic events simulated on the two sides, histories of asynchronous displacement were used, the results of the analyses reported in the following figures show a rather symmetrical result, at least in statistical terms. Fig. 6 shows longitudinal displacements

		PGA 1.60	PGA 2.80	PGA 5.70	2.8/1.6 = 1.75	5.7/1.6 = 2.94
Sic	Mean	0.470 m	0.680 m	1.53 m	1.44	3.26
	Standard deviation	0.108 m	0.159 m	0.341 m	1.47	3.15
	Fractile 95%	0.648 m	0.943 m	2.09 m	1.46	3.22
Cal	Mean	0.498 m	0.703 m	1.61 m	1.41	3.23
	Standard deviation	0.104 m	0.156 m	0.341 m	1.50	3.28
	Fractile 95%	0.734 m	1.09 m	2.20 m	1.30	2.25

Fig. 11. Transverse displacement of the bridge deck at a quarter of the bridge.
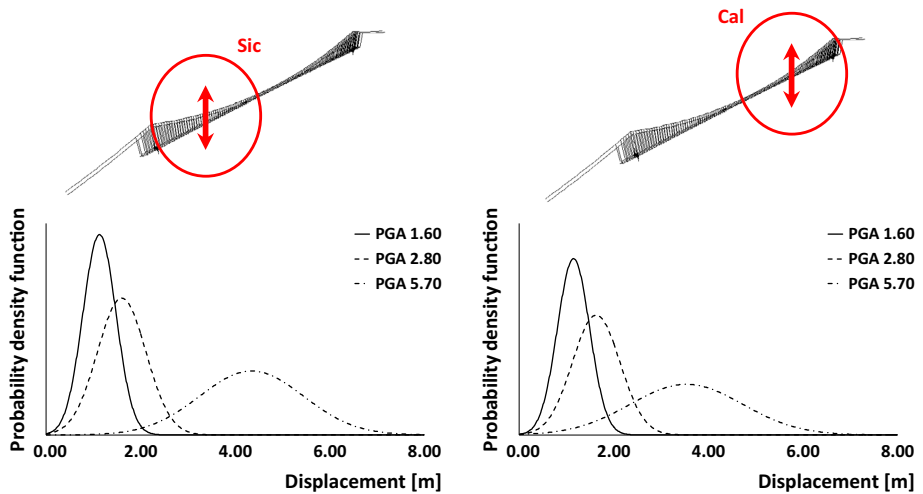
		PGA 1.60	PGA 2.80	PGA 5.70	2.8/1.6 = 1.75	5.7/1.6 = 2.94
Sic	Mean	1.13 m	1.60 m	3.45 m	1.44	3.26
	Standard deviation	0.351 m	0.514 m	1.10 m	1.46	3.13
	Fractile 95%	1.70 m	2.45 m	5.25 m	1.46	3.22
Cal	Mean	1.15 m	1.63 m	3.54 m	1.41	3.23
	Standard deviation	0.342 m	0.503 m	1.19 m	1.47	3.48
	Fractile 95%	1.72 m	2.46 m	5.50 m	1.30	2.25

Fig. 12. Vertical displacement of the bridge deck at a quarter of the bridge.

at joints located at the end of the bridge deck. Such values, above all the fractile at 95%, seem high and incompatible with the values reported in the specifications of the project with regard to the structure integrity (maximum permissible displacement equal to 1 m).

Fig. 10 shows the transverse displacement of the bridge deck near the towers. The values of displacement seem to be high. The fractile at 95% indicates a displacement of approximately 1 m with

the danger that seismic pounding can occur between the deck and the legs in the presence of strong earthquakes.

Figs. 11 and 12 show transverse and vertical displacements a quarter of the way across the bridge. It can be noted how the vertical displacement is more accentuated than the transverse displacement. A similar observation can be made for displacements at the centre of the bridge where the average value of the vertical displacement seems to be three times the average value of the
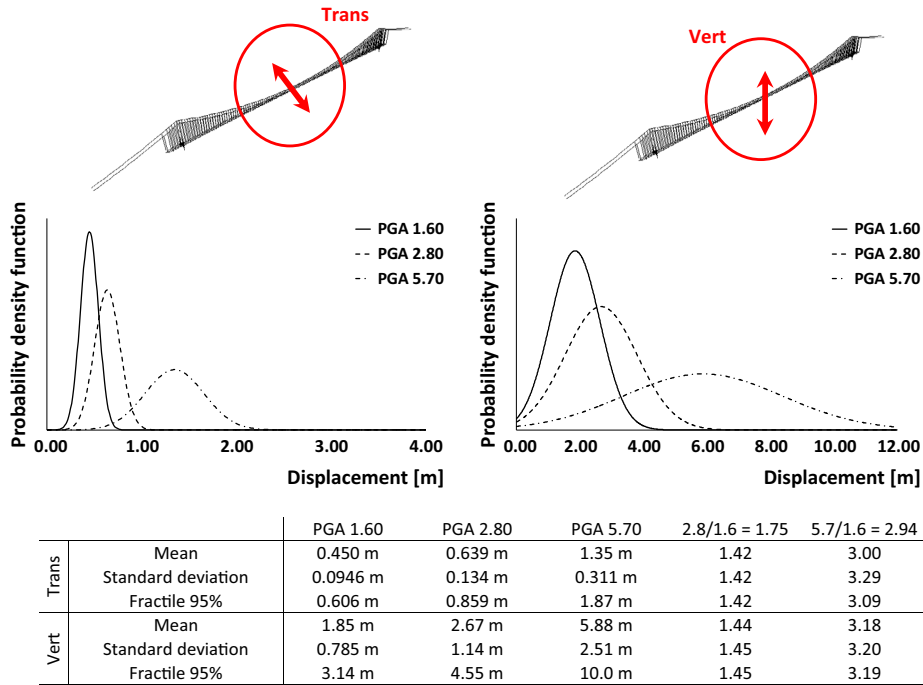
		PGA 1.60	PGA 2.80	PGA 5.70	2.8/1.6 = 1.75	5.7/1.6 = 2.94
Trans	Mean	0.450 m	0.639 m	1.35 m	1.42	3.00
	Standard deviation	0.0946 m	0.134 m	0.311 m	1.42	3.29
	Fractile 95%	0.606 m	0.859 m	1.87 m	1.42	3.09
Vert	Mean	1.85 m	2.67 m	5.88 m	1.44	3.18
	Standard deviation	0.785 m	1.14 m	2.51 m	1.45	3.20
	Fractile 95%	3.14 m	4.55 m	10.0 m	1.45	3.19

Fig. 13. Transverse and vertical displacement of the bridge deck at the centre of the bridge.

transverse displacement (Fig. 13). Observing the variances, it can also be noted that vertical displacements are more affected by uncertainties taken into consideration than transverse displacements.

Besides average values, it is interesting to note the impact of uncertainties on displacement parameters observed. It is known that the structural non-linear behaviour can amplify or reduce uncertainties. For example, as has already been shown in [44,45], the non-linearities and the time dependent behaviour (creep) of a box girder bridge are such that they can amplify initial uncertainties over time (divergent behaviour), while the behaviour of a stayed bridge tends to reduce them (convergent behaviour). Similarly the variance expected for the analyses carried out, if the behaviour of the bridge were not influenced by non-linearities, would be $1.44^2 = 2.09$ times the variance of the earthquake assumed as reference for the seismic scenario with PGA equal to 2.60 and $3.17^2 = 10.0$ m/s^2 times for the scenario with PGA equal to 5.70 m/s^2.

Aside from the longitudinal displacement, all the displacements analysed have values of variance close to these values, indicating the slight influence of non-linear behaviour of the bridge. The longitudinal displacement of the bridge deck seems instead to be strongly affected by non-linearities that cause average values and reduced dispersions compared with those that could be expected.

In a non-linear dynamics the different amplification of the uncertainties can be due to several factors such as the different stiffness of the bridge in various directions (vertical, longitudinal, transverse), the proximity of a seismic wave frequency to a natural frequency of vibration of the structure, the non-linear behaviour of the structure, etc. It is not easy to identify a single cause for such behaviour, and it is more likely that the results described are the synthesis of various phenomena that contribute in parallel to amplifying or reducing the influence of uncertainties.

Note that the absolute value of the displacements (S) is definitely a high value. However, such value must be considered in relation with the span (L) of the bridge (3300 m). Table 3 shows

the values of the ratio S/L for the transverse and vertical displacement of the bridge deck, at the centre of the bridge, related to the seismic scenarios with PGA 1.60 and 2.80 m/s^2 (scenarios in which it is important to guarantee the functionality of the structure).

The value of the ratio S/L for centre displacements seem to be acceptable. Only the vertical displacement valued to the fractile of 95% is slightly higher (1/725), but still acceptable considering the low probability of the event.

Fig. 14 shows the stress (the highest values that were evident during simulations) on the legs of the towers and on the main cable. In addition to the results of seismic simulations, the stress produced by the only permanent load is also reported in order to be able to carry out a comparison with an increase of stress due to seismic event.

With regard to the towers, Fig. 14 clearly shows how stress is strongly affected by the presence of the seismic action. Indeed, a passage from 116 MPa is highlighted due to the permanent load at an average value of 339 MPa in the event of earthquakes with PGA equal to 5.70 m/s^2. Considering an ultimate strength for steel equal to 510 MPa it can be observed that even for the scenario defined as "extreme" the stress results to be lower than the stress of collapse also for the relative value to the fractile at 95% (423 MPa).

It is interesting to note that with regard to stress due to the dead load solely on the legs of the towers, this is more or less constant while the seismic event produces a peak of stress at the base of the tower as well as at the third transverse of the same tower.

With regard to the main cables, Fig. 15 highlights how the stress increase that occurs during a seismic event is not particularly high and contained to 10% (for the average value) of the stress resulting from the sole permanent loads.

The maximum value of stress occurs at the saddle supports of the towers while the minimum level of stress occurs in the middle of the bridge. It should be noted that the areas of the cable mainly involved in the earthquake are those corresponding to the side spans where the trend of the maximum stress assumes an almost constant trend.
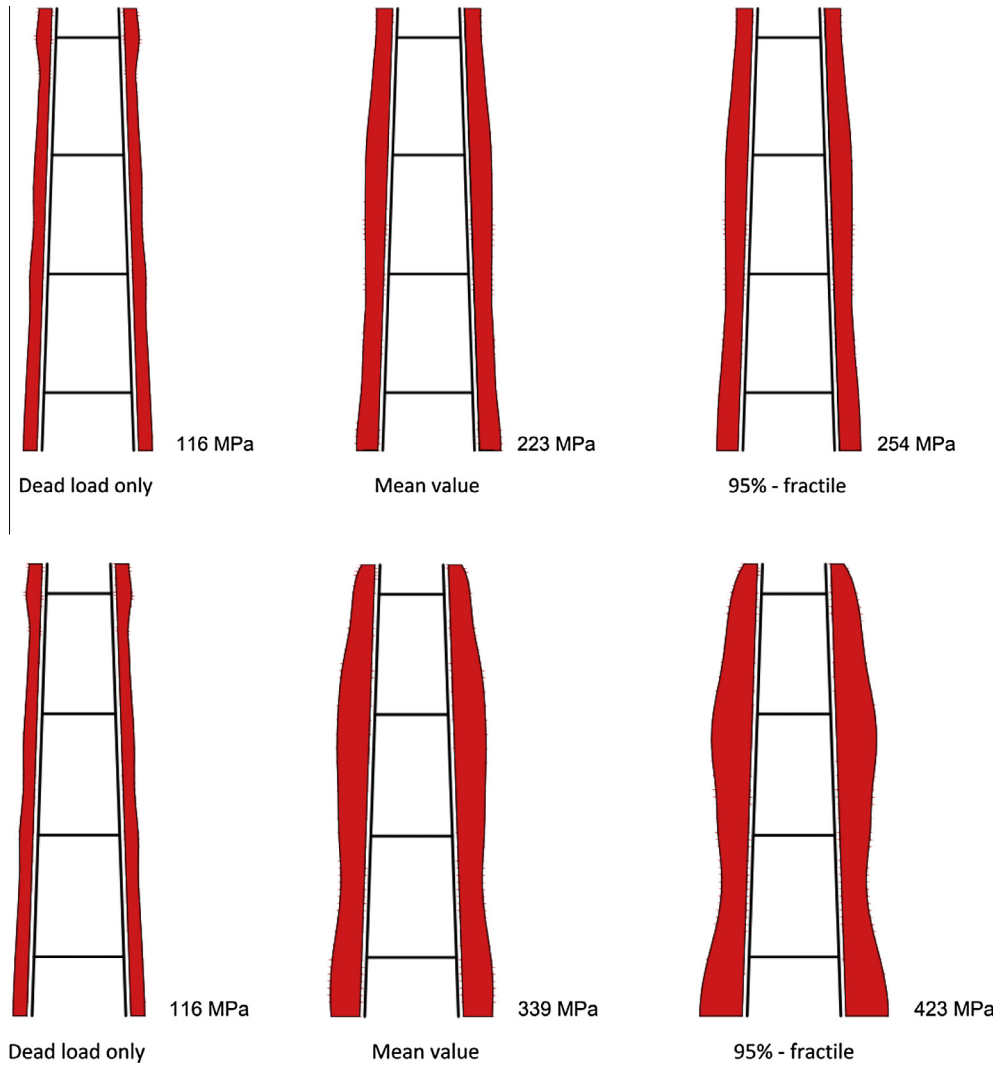
Fig. 14. Stress values in tower piers due to seismic load with PGA = 2.60 m/s^2 (top) and PGA = 5.70 m/s^2 (bottom).
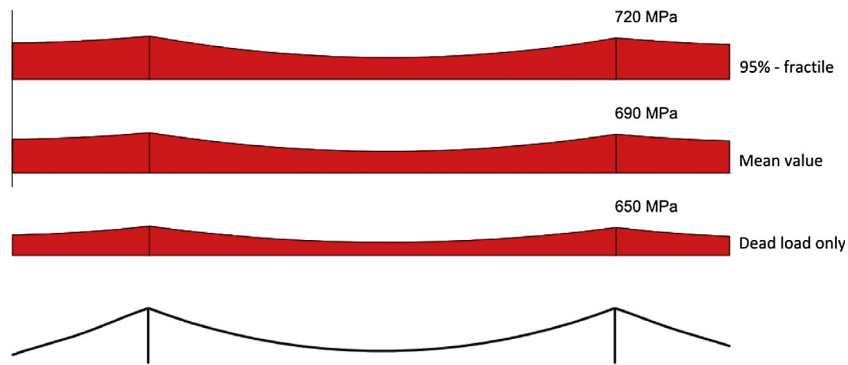

Fig. 15. Stress values in main cables due to seismic load with PGA = 5.70.

Table 3
Ratio displacement/span bridge for transverse and horizontal displacements valued at the centre of the bridge-deck for seismic scenarios having PGA 1.60 and 2.80 m/s^2.

	PGA 1.60		PGA 2.80	
	Mean	Fractile 95%	Mean	Fractile 95%
Transverse displacement of the bridge deck at the centre of the bridge	1/7333	1/5445	1/5164	1/3841
Vertical displacement of the bridge deck at the centre of the bridge	1/7184	1/1051	1/1235	1/725

5. Conclusions

In this paper a Monte Carlo seismic simulation was carried out on a large-span suspension bridge. The seismic motion, modelled as asynchronous spectrum-compatible histories of displacement, was evaluated using the ADINA software for a total of 50 seismic simulations for each PGA considered. Different seismic scenarios differ in terms of the form of temporal histories as well as the delay of the seismic action between various points of ground-structure contact.

The main results highlighted from the analyses are as follows:

- In the construction of artificial temporal histories necessary to simulate the seismic action, it was noted that passing from the accelerogram to the displacement time history (through a double integration) numerical errors occur (the higher they are the less precise the process of numerical integration) that make further correction based on the base-line method necessary.
- The convergence of position indices analysed (average and variance) takes place with different velocities. In order to obtain a convergence of the average value of variables studied, twenty analyses are sufficient, while it is necessary while more than fifty are required to obtain a good approximation of the statistical variance.
- Although for the simulated seismic events asynchronous histories of displacement were used, the results of the analyses reported show a rather symmetrical result, at least in statistical terms.
- Vertical displacements of the bridge deck are more influenced by the uncertainties taken into account, compared with transverse displacements.
- The uncertainties have less impact on longitudinal displacements of the bridge deck with regard to vertical and transverse directions.
- The values of longitudinal displacements at the expansion joint seem to be higher (higher than 1 m, if a fractile at 95% is considered and the seismic event of greater power considered).
- The values of transverse displacement of the bridge deck near the towers seem to be approximately 1 m with the danger that a seismic pounding can take place between the bridge deck and the tower legs in the presence of strong earthquakes.

In order to reduce the values of longitudinal displacement at the joint and transverse displacement at the towers, it may be necessary to introduce into the static scheme of the bridge certain passive control devices, transverse as well as longitudinal, that may connect the bridge deck to the towers.

Acknowledgements

References

[1] Sgambi L, Gkoumas K, Bontempi F. Genetic algorithms for the dependability assurance in the design of a long-span suspension bridge. Comput – Aided Civil Infrastruct Eng 2012;27(9):655–75.

[2] Petrini F, De Gaudenzi O, Gkoumas K. An energy harvesting application in a long span suspension bridge. In: Proc of the third international symposium on life-cycle civil engineering, Vienna, Austria, October 3–6; 2012.

[3] Simon HA. The structure of ill-structured problems. Artif Intell 1973;4:181–200.

[4] Der Kiureghian A, Ditlevsen O. Aleatory or epistemic? Does it matter? Struct Safety 2009;31(2):105–12.

[5] Barbato M, Petrini F, Unnikrishnan VU, Ciampoli M. Performance-based hurricane engineering (PBHE) framework. Struct Safety 2013;45:24–35. http://dx.doi.org/10.1016/j.strusafe.2013.07.002.

[6] Ciampoli M, Petrini F. Performance-based Aeolian risk assessment and reduction for tall buildings. Probab Eng Mech 2012;28:75–84.

[7] Barbato M, Tubaldi E. A probabilistic performance-based approach for mitigating the seismic pounding risk between adjacent buildings. Earthq Eng Struct Dynam 2013;42(8):1203–19.

[8] Garavaglia E, Sgambi L. The use of a credibility index in lifecycle assessment of structures. Struct Infrastruct Eng. doi: 10.1080/15732479.2014.896022; 2014 [in press].

[9] Sgambi L. Fuzzy theory based approach for three-dimensional nonlinear analysis of reinforced concrete two-blade bridge piers. Comput Struct 2004;82(13–14):1067–76.

[10] Beer M. Engineering quantification of inconsistent information. Int J Reliab Safety 2009;3(1–3):174–200.

[11] Dordoni S, Malerba PG, Sgambi L, Manenti S.Fuzzy reliability assessment of bridge piers in presence of scouring. In: Bridge maintenance, safety, management and life-cycle optimization – proc of the 5th international conference on bridge maintenance, safety and management, IABMAS 2010, Philadelphia, USA, July 2010 through 15 July 2010. CRC Press; 2010. p. 1388–95.

[12] Sgambi L. Handling model approximations and human factors in complex structure analyses. In: Proc of the 10th international conference on civil, structural and environmental engineering computing (CC05). Civil-Comp Press; 2005.

[13] Petrini F, Li H, Bontempi F. Basis of design and numerical modeling of offshore wind turbines. Struct Eng Mech 2010;36(5):599–624.

[14] Bontempi F. Basis of design and expected performances for the Messina Strait Bridge. In: Bridge 2006 – proc of the international conference on bridge engineering – challenges in the 21st century, November 2006, Hong Kong; 2006.

[15] Álvarez JJ, Aparicio AC, Jara JM, Jara M. Seismic assessment of a long-span arch bridge considering the variation in axial forces induced by earthquakes. Eng Struct 2012;34:69–80.

[16] Pergalani F, Compagnoni M, Petrini V. Evaluation of site effects using numerical analyses in Celano (Italy) finalized to seismic risk assessment. Soil Dynam Earthq Eng 2008;28(12):964–77.

[17] Di Capua G, Compagnoni M, Di Giulio G, Marchetti M, Milana G, Peppoloni S, Pergalani F, Sapia V. The seismic microzonation of level 3 of Sant'Agata Fossili (Northern Italy) based on a multidisciplinary approach. Ann Geophys 2014;57(1) [Article number S0189].

[18] Bommer JJ, Scott SG, Sarma SK. Hazard-consistent earthquake scenarios. Soil Dynam Earthq Eng 2000;19(4):219–31.

[19] Douglas J. What is a poor quality strong-motion record? Bull Earthq Eng 2003;1:141–56.

[20] Boore DM, Bommer JJ. Processing of strong-motion accelerograms: needs, options and consequences. Soil Dynam Earthq Eng 2005;25(2):93–115.

[21] Liu W, Liu Y. Commonly used earthquake source models. Geologos 2012;18(3):197–209.

[22] Rofooei FR, Mobarake A, Ahmadi G. Generation of artificial earthquake records with a nonstationary Kanai–Tajimi model. Eng Struct 2001;23(7):827–37.

[23] Musil M. Computation of synthetic seismograms in 2-D and 3-D media using the Gaussian beam method. Stud Geophys et Geodaet, Special Issue; 2002. p. 115–31.

[24] Amiri GG, Bagheri A, Seyed Razaghi SA. Generation of multiple earthquake accelerograms compatible with spectrum via the wavelet packet transform and stochastic neural networks. J Earthq Eng 2009;13(7):899–915.

[25] Cacciola P, Deodatis G. A method for generating fully non-stationary and spectrum-compatible ground motion vector processes. Soil Dynam Earthq Eng 2012;31(3):351–60.

[26] Ghaffarzadeh H, Izadi MM, Ghaffar NT. Neural network-based generation of artificial spatially variable earthquakes ground motions. Earthq Struct 2013;4(5):509–25.

[27] Ni SH, Xie WC, Pandey MD. Generation of spectrum-compatible earthquake ground motions considering intrinsic spectral variability using Hilbert–Huang transform. Struct Safety 2013;42:45–53.

[28] Shama AA. Simplified procedure for simulating spatially correlated earthquake ground motions. Eng Struct 2007;29(2):248–58.

[29] Abdel Raheem SE, Hayashikawa T, Dorka UE. Earthquake ground motion spatial variation effects on seismic response control of cable-stayed bridges. J Struct Eng 2009;55(A):709–18.

[30] Abdel Raheem SE, Hayashikawa T, Dorka UE. Ground motion spatial variability effects on seismic response control of cable-stayed bridges. Earthquake engineering and engineering vibration (Institute of Engineering Mechanics (IEM) China Earthquake Administration (CEA), MCEER-University at Buffalo, State University of New York); 2011, vol. 10, 1, p. 37–49.

[31] Yongxin W, Yufeng G, Dayong L. Simulation of spatially correlated earthquake ground motions for engineering purposes. Earthq Eng Eng Vib 2011;10:163–73.

[32] Lualdi M, Lombardi F. Effects of antenna orientation on 3-D ground penetrating radar surveys: an archaeological perspective. Geophys J Int 2013;196(2):818–27.

[33] Lualdi M, Lombardi F. Orthogonal polarization approach for three dimensional georadar surveys. NDT E Int 2013;60:87–99.

[34] Wang J, Hu S, Wei X. Effects of engineering geological condition on response of suspension bridges. Soil Dynam Earthq Eng 1999;18(4):297–304.

[35] Soyluk K, Dumanoglu AA. Comparison of asynchronous and stochastic dynamic responses of a cable-stayed bridge. Eng Struct 2000;22(5):435–45.

[36] Boissières HP, Vanmarcke EH. Spatial correlation of earthquake ground motion: non-parametric estimation. Soil Dynam Earthq Eng 1995;14:23–31.

[37] Bathe KJ. Finite element procedures in engineering analysis. Prentice-Hall; 1982.

[38] Sgambi L, Bontempi F. A fuzzy approach in the seismic analysis of long span suspension bridge. In: Proceedings of the 13th world conference on earthquake engineering, Vancouver, B.C., Canada, 1–6 August; 2004.

[39] Sgambi L, Gkoumas K, Bontempi F. Genetic algorithm optimization of precast hollow core slabs. Comput Concr 2014;13(3):389–409.

[40] Garavaglia E, Pizzigoni A, Sgambi L, Basso N. Collapse behaviour in reciprocal frame structures. Struct Eng Mech 2013;46(4):533–47.

[41] Gasparini D, Vanmarcke EH. Simulated earthquake motions compatible with prescribed response spectra, M.I.T. Department of Civil Engineering. Research report R76-4; 1976.

[42] Borsoi L, Ricard A. A simple accelerogram correction method to prevent unrealistic displacement shift. In: Proc 8th SMIRT Conference, Brussels; 1985.

[43] Ferreira MP, Negrão JH. Effects of spatial variability of earthquake ground motion in cable-stayed bridges. Struct Eng Mech 2006;23(3):233–47.

[44] Camossi G, Malerba PG, Sgambi L. Role of uncertainties on time dependent behaviour of prestressed and cable stayed concrete bridges. In: Bridge maintenance, safety, management and life-cycle optimization – proc of the 5th international conference on bridge maintenance, safety and management, IABMAS 2010, CRC Press: Philadelphia, USA; 2010. p. 1372–9.

[45] Malerba PG, Quagliaroli M, Sgambi L, Baraldi P. Time dependent behaviour of an elementary bridge model in presence of uncertainties. In: Bridge maintenance, safety, management, resilience and sustainability – proc of the sixth international conference on bridge maintenance, safety and management, IABMAS 2012, Stresa, Lake Maggiore, Italy, 8 July 2012 through 12 July 2012, CRC Press; 2012. p. 1771–8.